# Fatigue Life of a 2.5D C/SiC Composite Under Tension–Tension Cyclic Loading: Experimental Investigation and Sensitivity Analysis

Jingwei Yu[1,2]   Qingguo Fei[1,2⋆]   Peiwei Zhang[2]   Yanbin Li[1,2]   Qiang Chen[1,2]

([1]School of Mechanical Engineering, Southeast University, Nanjing 211189, China)

([2]Jiangsu Engineering Research Center of Aerospace Machinery, Southeast University, Nanjing 211189, China)

**ABSTRACT** Engineering structures made of ceramic matrix composites (CMCs) usually suffer from cyclic loads during service, which could lead to disastrous failures. This work focuses on the fatigue behavior of a 2.5D C/SiC composite under tension–tension cyclic loading. Experiments of the 2.5D C/SiC composite are firstly carried out to determine the fatigue lifetime of the material at different stress levels. The fracture surfaces examined by a scanning electronic microscope indicate that the damage mechanisms under cyclic loading are closely related to crack propagation, fiber/matrix interfacial degradation, and fiber breakage. Considering the damage evolution of fibers and interfacial resistance, a micromechanical model is adopted to describe the fatigue behavior of 2.5D C/SiC composite, and the numerical results are compared with the experimental results. Further, a sensitivity analysis is performed as a function of the interfacial shear stress, fiber Weibull modulus, and fiber strength. The calculation of sensitivity factors shows that the variations of the fiber Weibull modulus and fiber strength have the most significant influence and, thereafter, the variation of interfacial shear stress.

**KEY WORDS** Ceramic matrix composites (CMCs), 2.5D C/SiC composite, Fatigue, Mechanical properties, Sensitivity

## 1. Introduction

Due to the advantages of low density, high specific stiffness/strength, and high-temperature sustainability, ceramic matrix composites (CMCs) are highly sought-after engineering materials in aviation and aerospace industries [1–4]. Components made of CMCs are expected to experience fluctuating loads during service in most potential applications [5, 6]. The persistent cyclic loading can lead to damage accumulation and eventually catastrophic failure in CMCs [7, 8]. Therefore, it is essential to clearly understand the fatigue behavior of these CMCs.

Owing to the chemical vapor infiltration and liquid silicon infiltration method [9], the carbon-fiber-reinforced silicon carbide matrix (C/SiC) composite, as one of the most commonly used CMCs, has been allowed to fabricate with relatively low cost. In this context, various fiber preform architectures, such as unidirectional, two-dimensional (2D), and three-dimensional (3D) architectures, are developed

---

⋆ Corresponding author. E-mail: qgFei@seu.edu.cn

to improve the mechanical performance of composite structures. Among these C/SiC composites, the 2.5D C/SiC composites, which have excellent out-of-plane resistibility, the feasibility of mass manufacturing, and delamination resistance, are widely used in engineering applications. The existed studies regarding 2.5D C/SiC composites mainly focused on mechanical optimization, cost reduction, and ablation performance [10–14], while the investigations on the long-term mechanical performance of 2.5D C/SiC composites under cyclic loading are still limited. Some experiments were conducted to reveal the underlying damage mechanism during fatigue. Zhang et al. [15] studied the fatigue lifetime of 2.5D C/SiC composite under cyclic loading and observed that the fracture was closely related to the cracks originated from the crossover of fiber bundles. Li et al. [16] investigated the residual strength of 2.5D C/C-SiC composite, which was found to be improved after cyclic loading, especially for high-stress levels. Almeida et al. [17] examined the damage evolution of 2.5D C/C-SiC composite by acoustic emission monitoring, and the mechanisms of damage development during cyclic loading were analyzed.

The damage mechanisms of CMCs mainly conclude matrix crack growth, fiber/matrix interface sliding, and fiber breakage. Some theoretical research has been conducted to describe the damage mechanisms of CMCs. Curtin [18] applied the principles of weakest link statistics to represent the fiber breakage by using the global load-sharing (GLS) model. In the GLS model, the load released from the broken fibers is transferred to intact fibers, and the interfacial friction of the broken fibers within a slip length is considered. The GLS model is attractive for its elegance, ease of use, and reasonable predictions. Fruitful models have been developed based on the GLS model. Dutton et al. [19] considered the effects of stress concentration in fibers caused by matrix crack. Li [20] combined the GLS model with fracture mechanics approach to determine the fraction of broken fibers and interface debonded length during matrix cracking. Further, Li [21] considered the fatigue damage mechanisms including interface wear and fiber oxidation to determine the fatigue lifetime of CMCs. The above modeling works mainly focused on unidirectional, 2D, and 3D CMCs, while related work on the 2.5D CMCs is still limited.

A problem met when managing the fatigue of CMCs is the dispersion in the datasets obtained from experiments. Since the uncertainties and errors inherent in the material cannot be eliminated, the influences of these uncertain factors could be a potential risk factor during service. The key to solving the issue of reliable fatigue analysis is to establish a sensitivity analysis, which could evaluate the influence of uncertainties and pinpoint directions for optimum composite designs. The existed work regarding fatigue sensitivity analysis mainly focused on metallic materials [22, 23]. Related investigations on composite materials are limited. The fatigue behavior of CMCs is closely related to their micromechanical properties, such as the fiber/matrix interfacial resistance, fiber strength, etc. Hence, it is necessary to conduct a fatigue sensitivity analysis of these micromechanical properties.

In this work, the fatigue life of a 2.5D C/SiC composite under tension–tension cyclic loading was investigated. Experiments were firstly carried out to determine the fatigue lifetime of the material under cyclic loading. Then, the microstructures of fractured surfaces were characterized by a scanning electron microscope to study the damage mechanism. Further, a micromechanical model was used to describe the damage evolution and predict the fatigue life of the 2.5D C/SiC composite, and the numerical results were compared with the experiment data. A sensitivity analysis was finally performed to investigate the influence of some parameters such as interfacial shear stress, fiber strength, and fiber Weibull modulus on the fatigue life scenario.

## 2. Experimental Details

### 2.1. Materials

The 2.5D C/SiC composite was fabricated by the Shanghai Institute of Ceramics, People's Republic of China. The carbon fiber (T-300$^{TM}$) with a diameter of 7 $\mu$m was provided by Toray Industries, Inc. The low-pressure chemical vapor infiltration (CVI) method was employed to prepare the composite. Figure 1 shows the schematic of reinforcement in C/SiC composite, where the reinforcement is composed of layers of woven warp and weft yarns, and a set of needled yarns along the thickness direction with the step length of 5 mm. The material was fabricated identically for warp and weft directions. The fiber volume fraction and porosity of the material were nearly 40% and 8%, respectively. After the deposition of SiC, the contoured, edge-loaded test specimens were machined from the fabricated plates. The shape of the specimen agrees with the standard test method provided by the American
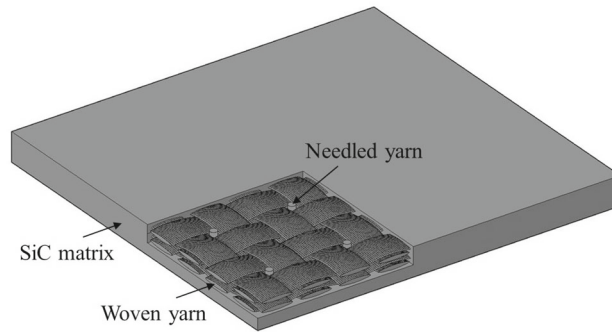
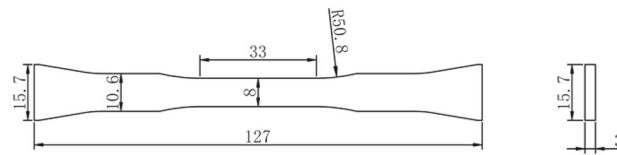Fig. 1. Schematic of reinforcement in 2.5D C/SiC composite



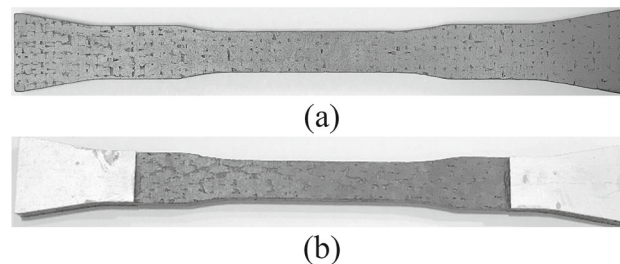Fig. 2. Dimensions of the 2.5D C/SiC specimen (in mm)



Fig. 3. Specimen for experiments: **a** virgin sample; **b** sample with aluminum alloy sheets

Society for Testing and Materials (ASTM) C1275, and the geometry of the specimen is shown in Fig. 2. It should be noted that the width of the specimen was widened to 8 mm to reduce the influence of the dispersion of material properties, such as the irregular voids [24, 25]. Other dimension parameters satisfy the requirements of ASTM.

### 2.2. Test Procedure

Monotonic tensile and tension–tension cyclic loading tests were conducted for the 2.5D C/SiC composite in the warp direction. The environment temperature and humidity were nearly 20 °C and 40%, respectively. All tests followed the standard test method provided by the ASTM C1259 and ASTM C1360. A servo-hydraulic mechanical testing machine (Instron 8802) equipped with water-cooled grips was used in the experiments. The gripping devices were designed according to the standard test method provided by the ASTM C1275. The passive grips acted through edge loading via the grip interface at the shoulder of the specimen shank. Aluminum alloy sheets were bonded to the shoulders of the specimen to avoid compressive failure in the gripped section during testing, as shown in Fig. 3. All cyclic tests were carried out in load control at the frequency of 2 Hz, with the stress ratio of 0.3. The smooth transitions between maximum and minimum stresses were given as sine waves. It was assumed that the fatigue run-out occurs at $10^6$ cycles (corresponding to 139 hours). Further, the fracture morphology of the specimen was examined by a scanning electronic microscope (FEI Inspect F50).
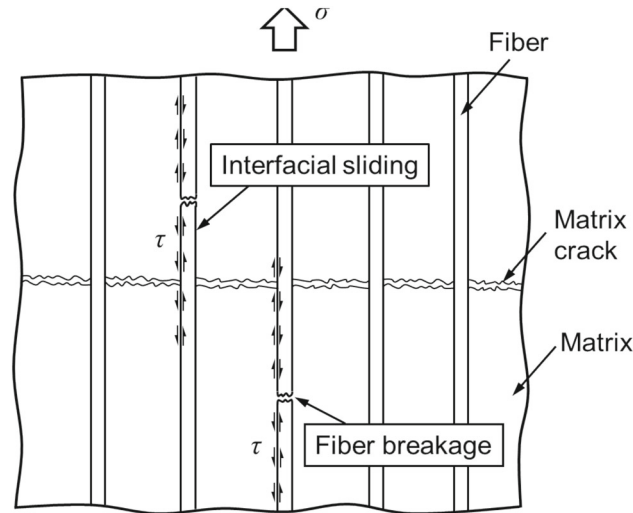
Fig. 4. Schematic of the stress distribution after matrix cracking

## 3. Theoretical Basis

### 3.1. Global Load-Sharing Model

For CMCs, the fracture strain of fibers is higher than that of the matrix, which leads to cracks in the matrix first, and then, fiber bridging sustains the load on the crack plane in tension. Figure 4 shows a schematic of stress distribution after matrix cracking. With the increasing load, the breakage occurs in weak fibers first. The interfaces between the broken fibers and the matrix are subjected to shear stress due to the different elongations between cracked matrix and bridging fibers, leading to interfacial debonding. In the debonded zone, the bridging fibers slide with friction around the matrix crack [26]. Consequently, the applied load is partially carried by intact fibers, and the remainder is carried by broken fibers within a slip length of the crack plane [18]. The effective coefficient of the fiber volume fraction in the loading direction, defined by Mei et al. [27], is introduced into the global load-sharing model as

$$\frac{\sigma}{\lambda_f V_f} = T(1-P) + T_{\text{b}} \cdot P \tag{1}$$

where $\sigma$ is the applied stress, $V_f$ is the volume fraction of fibers, $\lambda_f$ is the effective coefficient of the fiber volume fraction in the loading direction, $P$ is the fraction of broken fibers, $T$ is the load carried by intact fibers, and $T_{\text{b}}$ is the load carried by broken fibers.

The strength of fibers is related to the random distribution of flaws in fibers, where the failure probability of fiber is statistically described by the Weibull distribution [18]

$$P = 1 - \exp\left[-\left(\frac{T}{\sigma_c}\right)^{m+1}\right] \tag{2}$$

where the shape parameter $m$ describes the dispersion of measured strengths, and $\sigma_c$ is the characteristic strength of a single fiber of length $\delta_c$. The $\sigma_c$ and $\delta_c$ are, respectively, given by [18]

$$\sigma_c = \left(\frac{\sigma_0^m \tau L_0}{r}\right)^{1/(m+1)}, \, \delta_{\text{c}} = \left(\frac{\sigma_0 r L_0^{1/m}}{\tau}\right)^{m/(m+1)} \tag{3}$$

where $\sigma_0$ is the average stress to cause one failure in a fiber of length $L_0$, $\tau$ is the frictional sliding stress between the fiber and matrix, and $r$ is the fiber radius. The critical fraction of broken fibers is given as [18]

$$P_f = \frac{2}{m+2} \tag{4}$$

The average load carried by those broken fibers within a slip length of the crack plane is determined by

$$T_{\rm b}(x) \cdot \pi r^2 = \tau \cdot 2\pi r \cdot x \tag{5}$$

where $x$ is the sliding distance from the crack plane.

The total slip length $l_f$, which denotes the fiber stress required to reach the intact value, is given as

$$l_f = \frac{rT}{2\tau} \tag{6}$$

The probability distribution $f(x)$ that a break occurs at $x$ within $l_f$ is given as [28]

$$f(x) = \frac{1}{Pl_f} \left(\frac{T}{\sigma_c}\right)^{m+1} \times \exp\left[-\left(\frac{x}{l_f}\right)\left(\frac{T}{\sigma_c}\right)^{m+1}\right] \quad x \in [0, l_f] \tag{7}$$

Then, the average stress carried by broken fibers is determined as

$$T_{\rm b} = \int_0^{l_f} T_{\rm b}(x) \cdot f(x) \mathrm{d}x = T\left[\left(\frac{\sigma_c}{T}\right)^{m+1} - \frac{1-P}{P}\right] \tag{8}$$

## 3.2. Damage Evolution

For CMCs, the crack of matrix usually leads to the debonding of the interface at the crack front, accompanied by frictional sliding along the detached interface. The interfacial wear mechanism under cyclic loading is related to the asperity height reduction as the surface sliding [29], where the contact of rough surfaces develops by aging higher contact areas. The wear damage along the fiber/matrix interface leads to the decrease in interfacial shear stress [30], and the variation of interfacial shear stress with loading cycles is described by [31]

$$\frac{\tau(N) - \tau_0}{\tau_s - \tau_0} = 1 - \exp\left(-\omega N^\lambda\right) \tag{9}$$

where $\tau_0$ is the initial interfacial shear stress, $\tau_{\rm s}$ is the steady-state interfacial shear stress, $\tau(N)$ is the interfacial shear stress corresponding to the $N$th loading cycle, and $\omega$ and $\lambda$ are the empirical parameters.

Under cyclic loading, the progress of unloading and reloading could also lead to the damage in carbon fibers [32], where the damage evolution of fibers is described by [21]

$$\sigma_0(N) = \sigma_0\left[1 - p_1 (\log N)^{p_2}\right] \tag{10}$$

where $p_1$ and $p_2$ are the empirical parameters.

The fraction of broken fibers corresponding to the $N$th loading cycle can then be determined by substituting Eq. (9) and Eq. (10) in Eq. (2) [33]

$$P(N) = 1 - \exp\left\{-\left(\frac{T}{\sigma_c}\right)^{m+1}\left(\frac{\sigma_0}{\sigma_0(N)}\right)^m \left(\frac{\tau_0}{\tau(N)}\right)\right\} \tag{11}$$

The load carried by those broken fibers within a slip length of the crack plane under cyclic loading is determined by

$$T_{\rm b}(x) \cdot \pi r^2 = \tau(N) \cdot 2\pi r \cdot x \tag{12}$$

The total slip length $l_f$ and the probability distribution $f(x)$ that a break occurs at $x$ under cyclic loading are, respectively, determined as

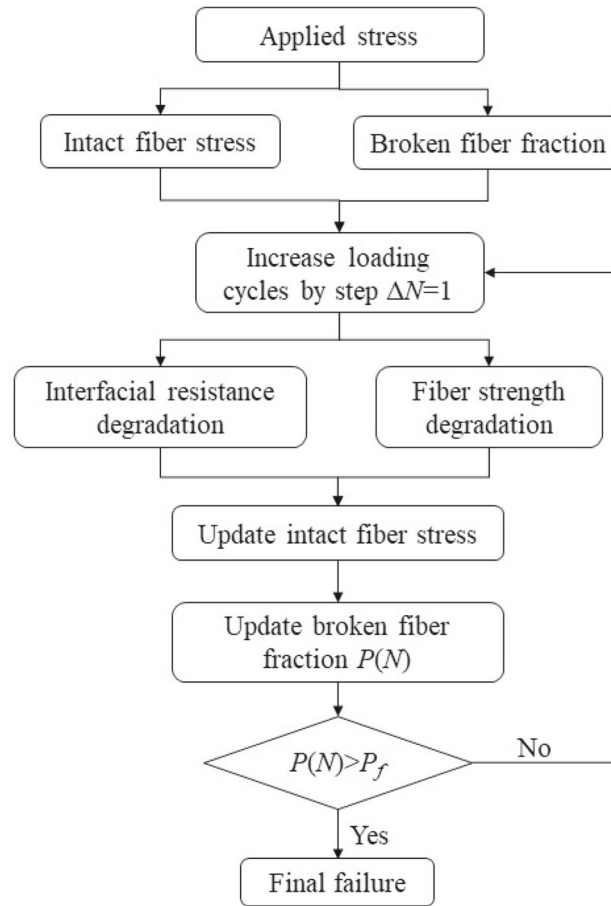$$l_f = \frac{rT}{2\tau(N)} \tag{13}$$

Fig. 5. Schematic diagram of the model to predict the fatigue life of CMCs

$$f(x) = \frac{1}{P(N)l_f} \left(\frac{T}{\sigma_c}\right)^{m+1} \left(\frac{\sigma_0}{\sigma_0(N)}\right)^m \frac{\tau_0}{\tau(N)} \times$$
$$\exp\left[-\left(\frac{x}{l_f}\right)\left(\frac{T}{\sigma_c}\right)^{m+1}\left(\frac{\sigma_0}{\sigma_0(N)}\right)^m \frac{\tau_0}{\tau(N)}\right] \quad (x \in [0, l_f]) \tag{14}$$

Then, the average stress carried by broken fibers is given by

$$T_{\mathrm{b}}(N) = \int_0^{l_f} T_{\mathrm{b}}(x) \cdot f(x)\mathrm{d}x = T\left[\left(\frac{\sigma_c}{T}\right)^{m+1}\left(\frac{\sigma_0(N)}{\sigma_0}\right)^m \frac{\tau(N)}{\tau_0} - \frac{1}{P(N)}\left(1 - P(N)\right)\right] \tag{15}$$

### 3.3. Fatigue Life

Under cyclic loading, the relationship between the applied load, the fraction of broken fibers, and the number of loading cycles in the GLS model is determined by substituting Eq. (11) and Eq. (15) in Eq. (1)

$$\sigma = \lambda_f V_f \cdot \left(\frac{\sigma_0(N)}{\sigma_0}\right)^m \frac{\tau(N)}{\tau_0} \cdot \frac{\sigma_c^{m+1}}{T^m} \cdot P(N) \tag{16}$$

where the interfacial shear stress and fiber strength can be determined by Eqs. (9) and (10), respectively. The stress carried by intact fibers can be determined by substituting Eqs. (9) and (10) in Eq. (16), and the fraction of broken fibers is obtained by substituting the intact fiber stress in Eq. (11).

The schematic diagram of the model to predict fatigue life is shown in Fig. 5. At a given stress, the initial intact fiber stress and fraction of broken fibers can be determined using the GLS model.

Table 1. **Test results of 2.5D C/SiC composite under monotonic/cyclic loading**

| | Sample | Maximum stress | Percentage of (MPa) | Cycles to failure UTS (%) | Time to failure (h) |
|---|---|---|---|---|---|
| Monotonic tensile loading | T-1 | 268.5 | | | |
| | T-2 | 262.7 | – | – | – |
| | T-3 | 246.7 | | | |
| Tension–tension cyclic loading | C-1 | 245.0 | 94.5 | $2.72\times 10^4$ | 3.78 |
| | C-2 | 224.6 | 86.6 | $4.95\times 10^4$ | 6.88 |
| | C-3 | 223.8 | 86.3 | $5.40\times 10^4$ | 7.50 |
| | C-4 | 218.0 | 84.1 | $1.84\times 10^4$ | 2.56 |
| | C-5 | 207.9 | 80.1 | $4.08\times 10^5$ | 56.67 |
| | C-6 | 202.5 | 78.1 | $> 10^6$ | $> 139$ |

Under cyclic loading, the number of loading cycles is increased by step $\Delta N$=1. For each increment, the interfacial shear stress and fiber strength corresponding to the $N$th loading cycle are determined. Then, the stress carried by intact fibers and the fraction of broken fibers for each loading cycle are updated. The process is repeated until the fraction of broken fibers exceeds the critical value, which is assumed to trigger the unstable crack propagation and eventual failure.

# 4. Results

### 4.1. Experimental Data

The test results of the 2.5D C/SiC composite under monotonic tensile loading and cyclic loading are shown in Table 1, which exhibit a certain degree of data scatter. This dispersion can be partly explained by the inherent uncertainties of the material, such as the uncertain constituent material properties and the irregular flaws. The average strength of the material equals 259.3 MPa under monotonic tensile loading. Figure 6 shows the typical stress–strain curve of 2.5D C/SiC composite under monotonic tensile loading. The composite exhibits linear behavior near the origin. As the load increases continuously, cracks arise and propagate in the matrix. The matrix cannot bear the applied load when matrix cracking reaches a certain level, and most of the loads are transferred to fibers. The uncorrelated rupture of fibers results in nonlinear behavior, and a decreasing tangent modulus is observed in the stress–strain curve.

Under cyclic loading, the number of loading cycles to failure depends on the applied stress level. The fatigue life tends to be longer at a lower applied stress level. The fatigue run-out ($10^6$ cycles) is achieved in case when the applied maximum stress is decreased to 202.5 MPa, which corresponds to 78.1% of the average ultimate tensile strength (UTS). This shows high fatigue resistance of the 2.5D C/SiC composite under tension–tension cyclic loading at room temperature.

### 4.2. Microstructures

The fracture morphology of the specimen was examined by a scanning electronic microscope (FEI Inspect F50) to investigate the damage in 2.5D C/SiC composite. Damage modes including the debonding in transverse fiber bundles and pull-out of longitudinal fiber bundle segment can be observed at the fracture surfaces. Under monotonic tensile loading, the fracture surface is relatively smooth, where compact fiber bundles with few single fiber pull-outs can be found, as shown in Fig. 7a, b. Only a few interfacial detachments between fibers and the matrix can be observed among longitudinal fibers, indicating a strong interfacial resistance between fibers and the matrix.

Compared with the monotonic-loading specimens, the fracture surfaces of cyclic-loading specimens are relatively rough, where the pull-out of amounts of single fibers can be observed, as shown in Fig. 7c, d. The interfacial detaching indicates weak interfacial resistance between fibers and the matrix. The process of unloading–reloading reduces the sliding resistance of the interface and aggravates the detaching between fibers and the matrix. This enables the fibers to slide along the interface and results in a longer fiber pullout length. The random distribution of flaws in fibers could lead to various pullout lengths.
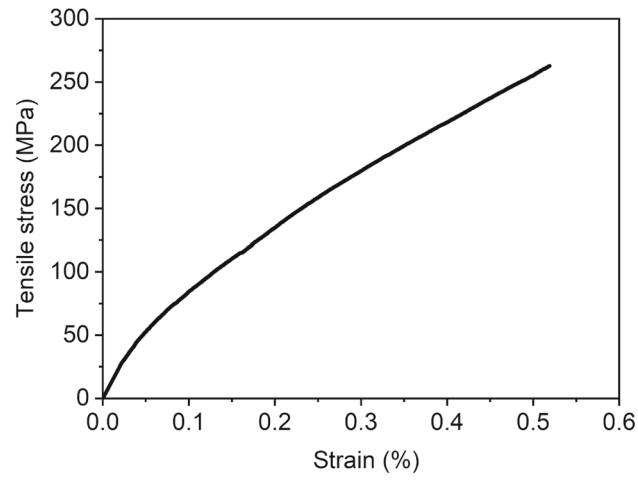
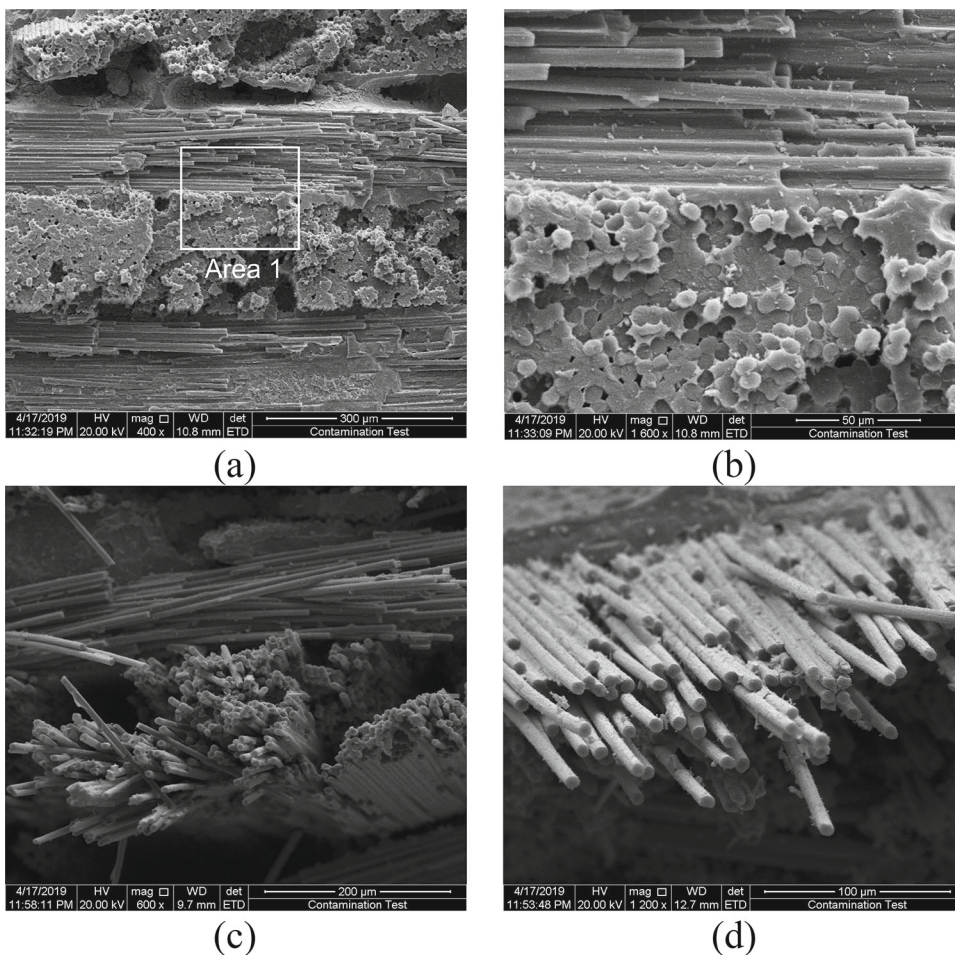Fig. 6. Typical tensile stress–strain curve of the 2.5D C/SiC composite



Fig. 7. SEM micrographs of fracture morphology: **a** monotonic-loading sample; **b** the magnification of Area 1; **c** cyclic-loading sample; **d** pullout of fibers

Table 2. **Material parameters in life prediction model**

| $V_f$ | $\lambda_f$ | $\tau_0$ [34] (MPa) | $\tau_s$ [34] (MPa) | $\sigma_0$ (MPa) | $L_0$ (mm) | $R$ (μm) | $m$ | $\omega$ [34] | $\lambda$ | $p_1$ | $p_2$ |
|---|---|---|---|---|---|---|---|---|---|---|---|
| 40% | 0.475 | 20 | 8 | 520 | 25 | 3.5 | 3.08 | 0.001 | 0.67 | 0.005 | 0.54 |


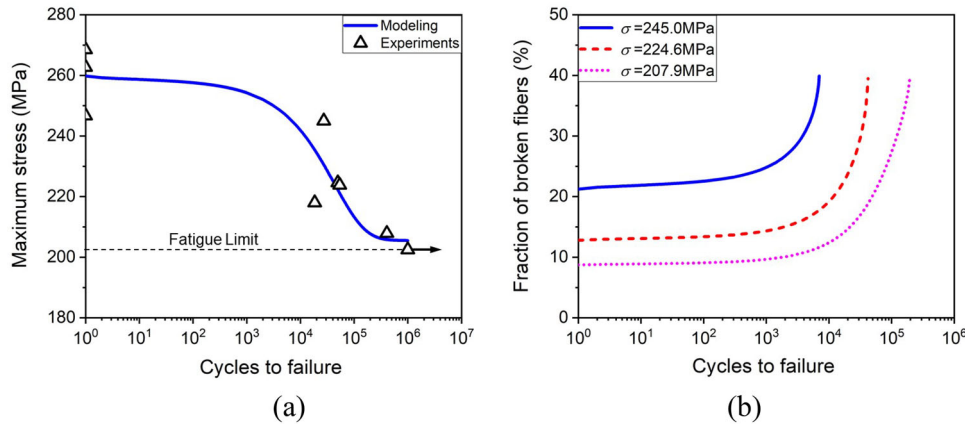
Fig. 8. Modeling results of the 2.5D C/SiC composite: **a** *S-N* curve; **b** fraction of broken fibers versus number of loading cycles to failure

### 4.3. Model Calibration

The micromechanical model described in Sect. 3.3 was adopted to describe the fatigue behavior of the 2.5D C/SiC composite. The related parameters are listed in Table 2. The shape parameter $m$ was determined by the GLS model. The empirical parameter $\omega$ was determined according to Li's work [34]. Then, the empirical parameter $\lambda$ was determined by one set of fatigue test data. Empirical parameters $p_1$ and $p_2$ were determined by the fatigue limit stress obtained by run-out test. The modeling results are shown in Fig. 8. The fit curve was in good agreement with the experimental results in terms of trend, while the experimental points did not perfectly match with the prediction line, as shown in Fig. 8a.

The fatigue lifetime is closely related to the applied stress level. According to the GLS model, a higher stress level leads to more fiber breakage, which means a higher fraction of broken fibers. Therefore, the fatigue life is relatively short at a high stress level. The frictions of broken fibers for different test stress levels ($\sigma$=207.9 MPa, 224.6 MPa, 245.0 MPa) are shown in Fig. 8b. Due to the damage in fibers and fiber/matrix interface, the fiber strength and interfacial shear stress decrease with the increasing number of loading cycles. The reduction in the loading capacity of fiber/matrix interface causes more loads to transfer to fibers. Consequently, more breakage occurs in fibers, and the fraction of broken fibers increases until exceeding the critical value.

## 5. Sensitivity Analysis and Discussions

Any fatigue strength property is affected by a certain level of scatter. Sensitivity analysis enables a consideration of the uncertainties inherent in the assessment, such as the scatter of material parameters and the uncertainties in the prediction model. To elucidate the influence of these uncertainties on the estimated fatigue life, different modeling options were performed. Only one parameter was investigated at one time, while others were kept constant. The outcome is expected to support a reliable life in fatigue assessment.

### 5.1. The Influence of Interfacial Shear Stress on Fatigue Life

Consider first the uncertainty of initial interfacial shear stress, where $\tau_0$=24 MPa, 20 MPa, 16 MPa (20%, 0, $-20\%$ deviations of the base value in Table 2) are taken into account, as shown in Fig. 9. More than half of the test data points fall within a variation of 20%. When the applied maximum stress is 240 MPa, the fatigue life corresponding to an initial interfacial shear stress of 20 MPa is equal to 12162 cycles. An increment (20%) of the shear stress produces an increment (87%) of the fatigue
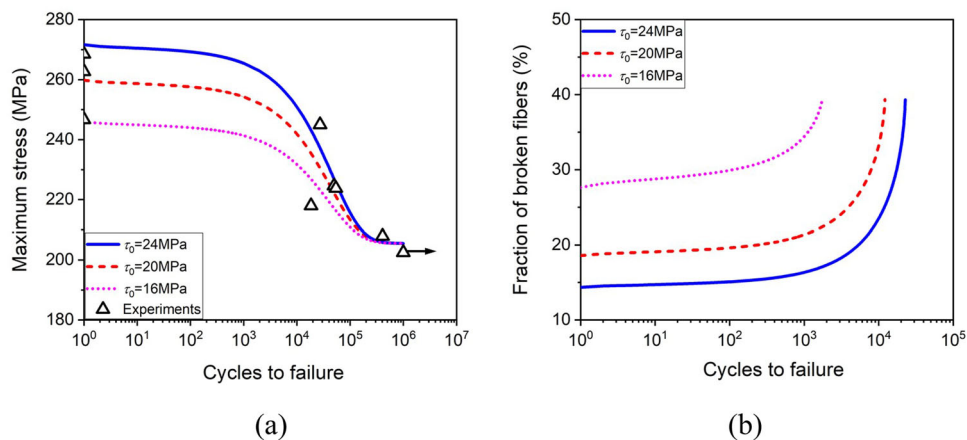
Fig. 9. **a** *S-N* curve; **b** fractions of broken fibers corresponding to different initial interfacial shear stresses
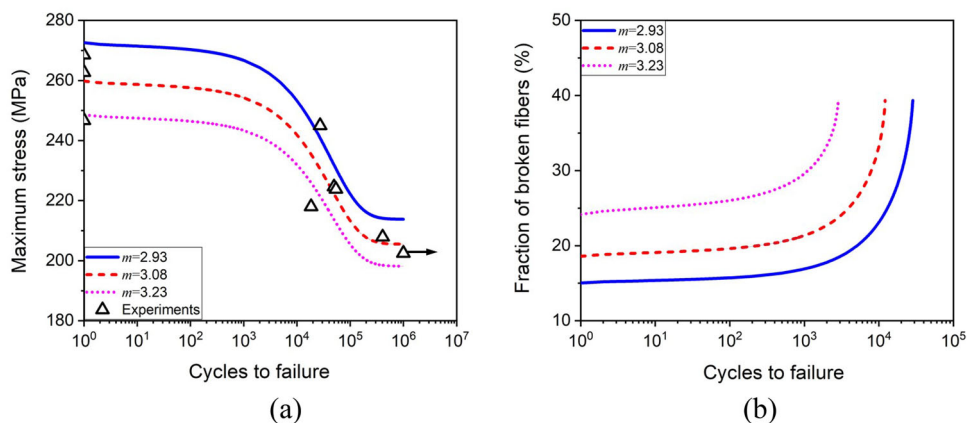


Fig. 10. **a** *S-N* curve; **b** fractions of broken fibers corresponding to different fiber Weibull moduli

life up to 22777 cycles. Due to the increase in initial interfacial shear stress, more loads are carried by the interface and the load transferred to fibers decreases. Therefore, more fibers survive and a lower fraction of broken fibers is achieved. On the contrary, the decrease in the shear stress leads to a higher fraction of broken fibers and then a reduction in fatigue life. A reduction (20%) in initial interfacial shear stress leads to a reduction (86%) in the fatigue lifetime to 1746 cycles. This clearly shows the significant sensitivity of the fatigue lifetime to initial interfacial shear stress.

### 5.2. The Influence of Fiber Weibull Modulus on Fatigue Life

The properties of fibers in CMCs are affected by various defects, where the fiber strength can be statistically described by the Weibull distribution. According to the study carried out by Curtin [18], the value of Weibull modulus $m$ is approximately located in a range of 2.7–3.9 for CMCs. In this study, the Weibull moduli equaling 2.93, 3.08, and 3.23 (5%, 0, −5% deviations of the base value in Table 2) are considered, as shown in Fig. 10. The test data points are mainly enveloped within the ±5% variation boundaries. When the applied maximum stress is 240 MPa, the fatigue lifetime corresponding to $m$ of 3.08 is 12162 cycles. A reduction (5%) in the Weibull modulus of 2.93 produces an increment (138%) in the fatigue lifetime up to 28914 cycles, and an increment (5%) in the Weibull modulus of 3.23 leads to a reduction (77%) in the fatigue lifetime to 2782 cycles. According to Eq. (2), a higher Weibull modulus leads to a higher fraction of broken fibers at the same applied stress and then to a lower fatigue lifetime. This result shows that a very small variation of the Weibull modulus leads to a large variation of fatigue lifetime.
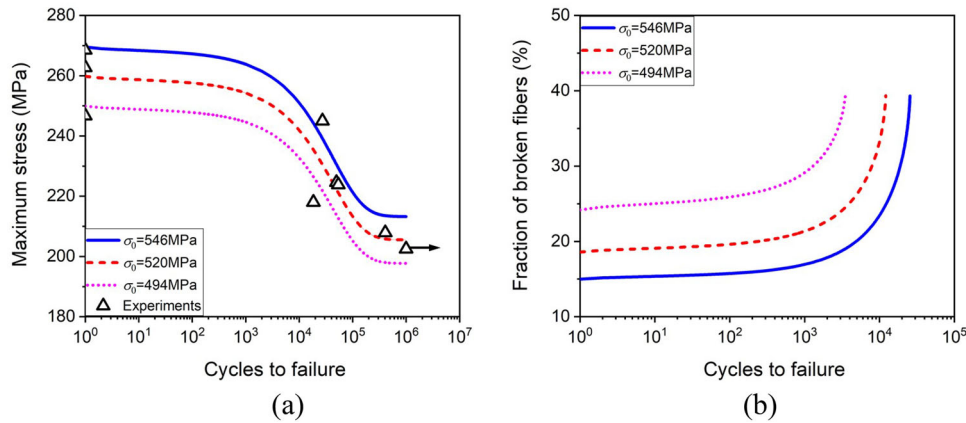
Fig. 11. **a** $S$-$N$ curve; **b** fractions of broken fibers corresponding to different fiber strengths

### 5.3. The Influence of Fiber Strength on Fatigue Life

Consider finally the variation of the fiber strength as a function of the sensitivity analysis. The fiber reference strengths of 494, 520 and 546 MPa (5%, 0, −5% deviations of the base value in Table 2) are considered, as shown in Fig. 11. More than half of the experimental data points are located in the scatter band of ±5%. When the applied maximum stress is 240 MPa, the fatigue lifetime corresponding to the fiber strength of 520 MPa is again equal to 12162 cycles. A reduction (5%) in the fiber strength to 494 MPa leads to a reduction (71%) in the fatigue lifetime to 3499 cycles. Due to the strength reduction, fewer fibers survive under the same applied load and a higher fraction of broken fibers is achieved. On the contrary, an increment (5%) in the fiber strength leads to an increment (111%) in the fatigue lifetime to 25612 cycles. This shows that the fatigue lifetime is very sensitive to fiber strength.

## 6. Conclusions

The CMCs are widely used in engineering structures suffering from cyclic loads. In this work, the fatigue behavior of a 2.5D C/SiC composite was investigated by experiments and modeling analysis. Experiments were performed to obtain the strength and fatigue life of the composite at different stress levels. The test results indicate that the 2.5D C/SiC composite has excellent fatigue resistance. The fatigue limit (run-out of $10^6$ cycles) for the 2.5D C/SiC composite is 202.5 MPa, which corresponds to 78.1% of its ultimate tensile strength. The damage mechanisms were investigated by observing the fracture morphology. Results show that the fiber/matrix interface debonding, sliding, and pullout of fibers in tension–tension fatigue tests are more obvious than those in monotonic tension tests, which indicate the serious degradation in interfacial resistance under cyclic loading.

A micromechanical model considering the damage evolution of fibers and interface, was adopted to describe the fatigue of the 2.5D C/SiC composite, and was then validated by the experimental data. Further, a sensitivity analysis was performed to investigate the dispersion in experimental datasets. The influence of interfacial shear stress, fiber strength, and Weibull modulus on the fatigue lifetime was studied. The results indicate that fatigue life is highly sensitive to fiber Weibull modulus and fiber strength. Even a small variation of the fiber Weibull modulus or fiber strength can result in a significant variation on fatigue life. Thereafter, the influence of interfacial shear stress cannot be ignored.

## References

[1] Yin XW, Cheng LF, Zhang LT, Travitzky N, Greil P. Fibre-reinforced multifunctional SiC matrix composite materials. Int Mater Rev. 2017;62(3):117–72.

[2] Chang YJ, Jiao GQ, Zhang KS, Wang B, Ju JW. Application and theoretical analysis of C/SiC composites based on continuum damage mechanics. Acta Mech Solida Sin. 2013;26(5):491–9.

[3] Chen Q, Fei QG, Devriendt H, Wu SQ, Pluymers B, Desmet W. The dynamic bending analysis of plates under thermal load using an efficient wave-based method. Thin Wall Struct. 2020;149:106421.

[4] Huang W, Wang M, Hu Z, Wang LL, Cao JX, Kong DW. Experimental and numerical investigation on strain rate-dependent tensile behavior of ZrB2-SiC ceramic composite. Acta Mech Solida Sin. 2020;34(1):137–48.

[5] Zhou YD, Hang XC, Wu SQ, Fei QG, Trisovic N. Frequency-dependent random fatigue of panel-type structures made of ceramic matrix composites. Acta Mech Solida Sin. 2017;30(2):165–73.

[6] Yu JW, Fei QG, Zhang PW, Li YB, Zhang DH, Guo F. An innovative yield criterion considering strain rates based on Von Mises stress. J Press Vess-T Asme. 2020;142(1).

[7] Zhang YF, Tang C, Zhang YB, Liang ZZ. Fractural process and toughening mechanism of laminated ceramic composites. Acta Mech Solida Sin. 2007;20(2):141–8.

[8] Wang M, Zhang PW, Fei QG, Guo F. Modified micro-mechanics based multiscale model for progressive failure prediction of 2D twill woven composites. Chinese J Aeronaut. 2020;33(7):2070–87.

[9] Tang SF, Hu CL. Design, preparation and properties of carbon fiber reinforced ultra-high temperature ceramic composites for aerospace applications: a review. J Mater Sci Technol. 2017;33(2):117–30.

[10] Chen LJ, Yao XF, Cen S. Predictions of elastic property on 2.5D C/SiC composites based on numerical modeling and semi-analytical method. Compos Part B-Eng. 2015;74:53–65.

[11] Zhang CY, Zhao MM, Liu YS, Wang B, Wang XW, Qiao SR. Tensile strength degradation of a 2.5D-C/SiC composite under thermal cycles in air. J Eur Ceram Soc. 2016;36(12):3011–9.

[12] Jiang D, Li YB, Fei QG, Wu SQ. Prediction of uncertain elastic parameters of a braided composite. Compos Struct. 2015;126:123–31.

[13] Fang D, Chen ZF, Song YD, Sun ZG. Morphology and microstructure of 2.5 dimension C/SiC composites ablated by oxyacetylene torch. Ceram Int. 2009;35(3):1249–53.

[14] Chen SF, Fei QG, Jiang D, Cao ZF. Determination of thermo-elastic parameters for dynamical modeling of 2.5D C/SiC braided composites. J Mech Sci Technol. 2018;32(1):231–43.

[15] Zhang CY, Wang XW, Liu YS, Wang B, Han D, Qiao SR, et al. Tensile fatigue of a 2.5D-C/SiC composite at room temperature and 900 degrees C. Mater Design. 2013;49:814–9.

[16] Li Y, Xiao P, Luo H, Almeida RSM, Li Z, Zhou W, et al. Fatigue behavior and residual strength evolution of 2.5D C/C-SiC composites. J Eur Ceram Soc. 2016;36(16):3977–85.

[17] Almeida RSM, Li Y, Besser B, Xiao P, Zhou W, Bruckner A, et al. Damage analysis of 2.5D C/C-SiC composites subjected to fatigue loadings. J Eur Ceram Soc. 2019;39(7):2244–50.

[18] Curtin WA. Theory of mechanical-properties of ceramic-matrix composites. J Am Ceram Soc. 1991;74(11):2837–45.

[19] Dutton RE, Pagano NJ, Kim RY, Parthasarathy TA. Modeling the ultimate tensile strength of unidirectional glass-matrix composites. J Am Ceram Soc. 2000;83(1):166–74.

[20] Li LB. Synergistic effects of fiber debonding and fracture on matrix cracking in fiber-reinforced ceramic-matrix composites. Mat Sci Eng a-Struct. 2017;682:482–90.

[21] Li LB. Damage development and lifetime prediction of fiber-reinforced ceramic-matrix composites subjected to cyclic loading at 1300 degrees C in vacuum, inert and oxidative atmospheres. Aerosp Sci Technol. 2019;86:613–29.

[22] Colombi P. Fatigue analysis of cemented hip prosthesis: damage accumulation scenario and sensitivity analysis. Int J Fatigue. 2002;24(7):739–46.

[23] Santus C, Taylor D, Benedetti M. Experimental determination and sensitivity analysis of the fatigue critical distance obtained with rounded V-notched specimens. Int J Fatigue. 2018;113:113–25.

[24] Wang M, Zhang PW, Fei QG, Guo F. Computational evaluation of the effects of void on the transverse tensile strengths of unidirectional composites considering thermal residual stress. Compos Struct. 2019;227:111287.

[25] Guo F, Fei QG, Li YB, Zhang PW, Wang M, Yu JW. Novel statistical analysis method for determining shear strength of C/C composite pin. Ceram Int. 2020;46(4):5262–70.

[26] Fantozzi G, Reynaud P. Mechanical behavior of SiC fiber-reinforced ceramic matrix composites. Comprehensive hard materials. Newnes, 2014;345–366.

[27] Mei H, Zhang LD, Xu HR, Cheng LF. Damage mechanism of a carbon fiber ceramic composite during the step-loading indentation and its effect on the mechanical properties. Compos Part B-Eng. 2014;56:142–8.

[28] Phoenix SL, Raj R. Scalings in fracture probabilities for a brittle matrix fiber composite. Acta Metall Mater. 1992;40(11):2813–28.

[29] Rouby D, Louet N. The frictional interface: a tribological approach of thermal misfit, surface roughness and sliding velocity effects. Compos Part a-Appl S. 2002;33(10):1453–9.

[30] Cho CD, Holmes JW, Barber JR. Estimation of interfacial shear in ceramic composites from frictional heating measurements. J Am Ceram Soc. 1991;74(11):2802–8.

[31] Evans AG, Zok FW, Mcmeeking RM. Overview No-118 - Fatigue of ceramic-matrix composites. Acta Metall Mater. 1995;43(3):859–75.
[32] Zhou YX, Baseer MA, Mahfuz H, Jeelani S. Statistical analysis on the fatigue strength distribution of T700 carbon fiber. Compos Sci Technol. 2006;66(13):2100–6.
[33] Li LB. Modeling the effect of oxidation on fatigue life of carbon fiber-reinforced ceramic-matrix composites at elevated temperature. Mat Sci Eng a-Struct. 2015;640:106–17.
[34] Li LB. Fatigue Life Prediction of carbon fiber-reinforced ceramic-matrix composites at room and elevated temperatures. Part: II experimental comparisons. Appl Compos Mater. 2015;22(6):961–72.